
Detecting ^3H with the BESS Spectrometer

Z. D. Myers¹, E. S. Seo¹, K. Abe⁴, K. Anraku^{2*}, M. Imori², T. Maeno^{4†}, Y. Makida³, H. Matsumoto², J. Mitchell⁵, A. Moiseev⁵, J. Nishimura², M. Nozaki⁴, J. F. Ormes⁵, S. Orito^{2§}, T. Sanuki², M. Sasaki⁵, Y. Shikaze⁴, R. E. Streitmatter⁵, J. Suzuki³, K. Tanaka³, T. Yamagami⁶, A. Yamamoto³, T. Yoshida³, K. Yoshimura³

(1) *IPST, University of Maryland College Park, MD, 20742, USA*

(2) *The University of Tokyo, Bunkyo, Tokyo, 113-0033, Japan*

(3) *High Energy Accelerator Research Organization (KEK), Tsukuba, Ibaraki 305-0801, Japan*

(4) *Kobe University, Kobe, Hyogo 657-8501, Japan*

(5) *NASA GSFC, Code 660, Greenbelt, MD20771, USA*

(6) *The Institute of Space and Astronautical Science (ISAS), Sagami-hara, Kanagawa 229-8510, Japan*

Abstract

For the past decade BESS (Balloon-borne Experiment with a Superconducting Spectrometer) has collected large quantities of cosmic-ray hydrogen and helium data. The instrument flown in 1998 was able to detect tritium between 0.10 GeV/n and 1.0 GeV/n. The timing resolution of 75 pico-seconds enabled the instrument to separate ^3H from ^2H with excellent mass resolution. The energy spectrum of ^3H and its abundance relative to parent nuclei were measured. The implications of these results on atmospheric ^2H corrections is discussed in this paper.

1. Introduction

The BESS instrument, which has been flown annually since 1993, was constructed as a high resolution instrument [1,2,9] to conduct searches for cosmic-ray anti-particles of novel primary origins and antimatter [5,6,8], and to take precise measurements of various cosmic ray components such as the isotopes of Hydrogen and Helium. The BESS 98 flight was carried out on July 29th, from Lynn Lake, Manitoba, Canada. The balloon floated for 22 hours. With the improved timing resolution of 75 ps, it was possible to clearly separate Hydrogen isotopes up to rigidities around 5 GV. The ^1H and ^2H spectra at the top of atmosphere were reported in [3,7]. In this balloon-borne experiment, accurate measurements of primary particles was hampered by secondary particles produced in the atmosphere. At low energies, the measured ^2H counts were dominated by

atmospheric secondaries and must be corrected in order to obtain the final ${}^2\text{H}$ spectrum at top of atmosphere. Tritium nuclei are secondary particles produced in the atmosphere primarily as a product of helium interacting air targets. We report our analysis of atmospheric ${}^2\text{H}$ and ${}^3\text{H}$ in this paper.

2. Data Analysis

The spectrum at the top of the atmosphere was obtained by correcting our measurements for the residual atmospheric overburden. Three physical processes of ionization, attenuation, and production were taken into account to calculate this secondary flux as shown in Wang et al. [12]. The transport equation used in this calculation is the same as Papini et al. [11]. While Webber's compiled data [13] were used as the input proton and helium spectra in Papini et al. [11], the measured BESS 98 proton and helium data were used in our calculation.

Since these events with negative rigidity are very rare compared to events with positive rigidity, a biased trigger was used to limit the number of positive events recorded at low energies. An unbiased set was collected, one out of 60 events for charge one ($Z = 1$) particles and one out of 25 events for charge two ($Z = 2$) particles. This "countdown" set was used in this analysis. The $Z = 1$ and $Z = 2$ candidates were separated by the ionization energy loss (dE/dx) of each event in the top time-of-flight counter. Cuts were applied to the $Z = 1$ candidates to ensure single track events. The purpose of the single-track selection is to eliminate events where nuclear interactions occurred inside the instrument. To ensure track quality and consistency further cuts were applied. After all the cuts, roughly 570,000 good $Z = 1$ events remained. The event selection efficiency was around 74% of all single-track events. The velocities of the remaining $Z = 1$ events as a function of rigidity are shown in Fig. 1. The events of ${}^1\text{H}$, ${}^2\text{H}$, and ${}^3\text{H}$ are clearly separated up to slightly above 5 GV. ${}^3\text{H}$ events are well separated from ${}^2\text{H}$ events between the energies of 0.10 and 1.0 GeV/n at the balloon altitude, i.e. atmospheric depth of 5 gcm^{-2} . Mass histograms for the detected ${}^3\text{H}$ events and their Gaussian fits are shown in Fig. 2. The area under the Gaussian function was used as a particle count for each energy bin. A similar selection process was done for $Z = 2$ events to separate ${}^3\text{He}$ and ${}^4\text{He}$ [4].

3. Results and Discussions

The estimated atmospheric deuterium secondaries were calculated with the BESS 98 hydrogen and helium input spectra [3,4] as was done by Wang et al. [12]. Our results are consistent with the calculations of Papini et al. [11] as shown in Fig. 3. Our calculation for BESS 98 (thick solid line) is in agreement with the calculation Papini et al. around the period of solar minimum (thin solid line).

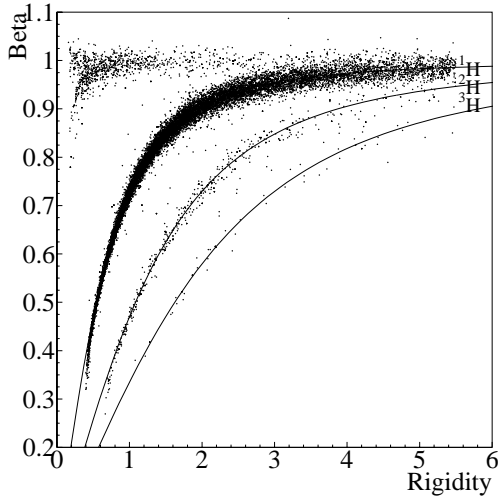


Fig. 1. The velocities of the $Z=1$ events as a function of rigidity. The solid curves show, from top to bottom, the theoretical relation between velocity and rigidity of hydrogen, deuterium, and tritium.

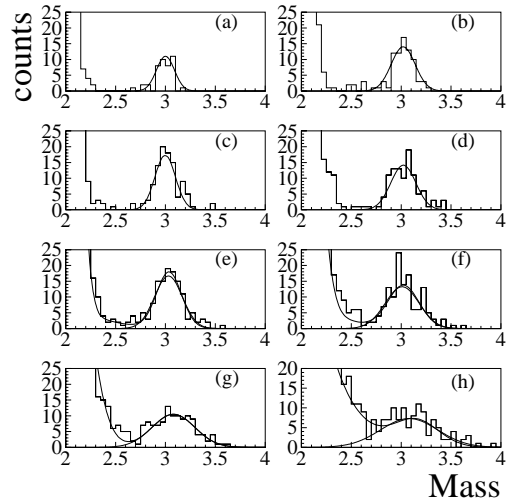


Fig. 2. Mass histograms of ^3H detected from BESS 98. ^3H was detected over specific energy ranges at the atmospheric depth of 5 g/cm^2 . The energy ranges in units of GeV/nucleon are as follows: (a) 0.10 - 0.13, (b) 0.13 - 0.18, (c) 0.18 - 0.24, (d) 0.24 - 0.32, (e) 0.32 - 0.42, (f) 0.42 - 0.56, (g) 0.56 - 0.75, (h) 0.75 - 1.0.

The measured ratio of ^3H at atmospheric depth of 5 gcm^{-2} to ^4He at the top of atmosphere was obtained in the energy ranges between 0.18 GeV/n and 1.0 GeV/n . The ^4He nuclei range out below 0.18 GeV/n due to ionization energy loss. The measured ratio as a function of energy was compared with Papini et al. [10], as shown in Fig. 4. The solid lines represent the $^3\text{H}/^4\text{He}$ calculation of Papini et al. for solar minimum. The dotted lines represent the same calculation for solar maximum. The BESS 98 data show excellent agreement with the predicted solar minimum curve for 5 gcm^{-2} atmospheric depth. At this grammage, the ratio of $^3\text{H}/^4\text{He}$ differs by roughly 20% between solar minimum and solar maximum [10]. The measured ^3H data are consistent with the atmospheric secondary calculations used to obtain the ^2H spectrum at the top of the atmosphere.

Acknowledgement

This work has been supported in the USA by NASA grant NAG5-5347, and in Japan by Grant-in-Aid for Scientific Research, MEXT and the Heiwa Nakajima Foundation.

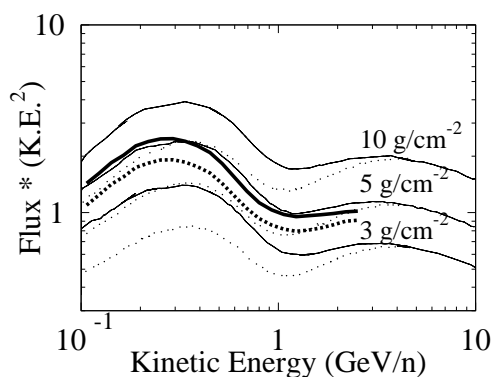


Fig. 3. Calculated flux of secondary ^2H at 5 g/cm^{-2} . The thick solid line represents the calculation from BESS 98. The thick dashed line represents the calculation from BESS 93 [12]. The solid lines represent Papini's ^2H calculation for solar minimum at different atmospheric depths (3, 5, & 10 g/cm^{-2}). The dotted lines represent the same calculation for solar maximum.

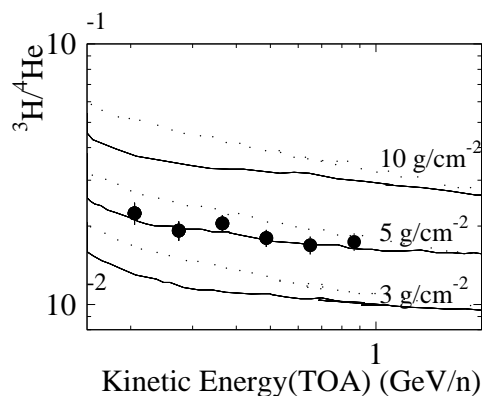


Fig. 4. The ratio of ^3H at 5 g/cm^{-2} to ^4He at the top of atmosphere (filled circles) as a function of energy. The solid line represents the Papini's $^3\text{H}/^4\text{He}$ calculation for solar minimum at different atmospheric depths (3, 5, & 10 g/cm^{-2}). The dotted line represents the same calculation for solar maximum.

* Present address: Kanagawa University, Yokohama, 221-8686, Japan

† Present address: CERN, CH-1211, Geneva 23, Switzerland

§ deceased

1. Ajima Y. et al., 2000, Nucl. Instr. Methods, A443, 71
2. Asaoka Y. et al., 1998, Nucl. Instr. Methods, A416, 236
3. Myers Z., et al. 2002, Advances in Space Research (submitted)
4. Myers Z., et al. 2003, Proc. 28th ICRC (submitted)
5. Orito, S. et al., 2000 Phys. Rev. Lett. 84 (6) 1078
6. Saeki T. et al., 1998 Phys. Lett. B 422, 319
7. Sanuki T. et al., 2000, AstroPhys. J. 545, 1135
8. Sasaki M. et al., Nucl. Phys. (Proc.Suppl.) B113 (2002) 202
9. Shikaze, Y. 2002, Nucl. Inst. Methods, A344, 596
10. Papini P., et al. 1993, Proc. 23rd ICRC, 1, 499
11. Papini P., et al. 1993, Proc. 23rd ICRC, 1, 503
12. Wang, J. Z., et al. 2001, ApJ 564, 244
13. Webber, W. R., 1973, Proc. 13th ICRC, 5, 3568